

Fault Detection and Isolation in Inertial Measurement Units Based on Bounding Sets

Sérgio Brás, *Student Member, IEEE*, Paulo Rosa, *Member, IEEE*, Carlos Silvestre, *Member, IEEE*, and Paulo Oliveira, *Senior Member, IEEE*

Abstract—This work addresses the problem of Fault Detection and Isolation (FDI) for navigation systems equipped with sensors providing inertial measurements and vector observations. Assuming upper bounded sensor noise, two strategies are proposed: i) the first one takes advantage of existing hardware redundancy, requiring at least five sensor measurements to isolate faults; ii) the second approach exploits the analytical redundancy between the angular velocity measurements and the vector observations, by resorting to set-valued observers (SVOs). Necessary and sufficient conditions on the magnitude of the faults are provided, in order to guarantee successful detection and isolation, when hardware redundancy is available. Due to the set-based construction of the methods, none of the solutions generates false detections and no decision threshold is required. Using a simulation scenario, the proposed strategies are compared with two alternatives available in the literature.

Index Terms—Aerospace, fault detection, fault isolation, navigation, set-valued observers.

NOMENCLATURE

The skew-symmetric operator in \mathbb{R}^3 is denoted by $(\cdot)_\times$ and satisfies $(\mathbf{v})_\times \mathbf{w} = \mathbf{v} \times \mathbf{w}$, $\mathbf{v}, \mathbf{w} \in \mathbb{R}^3$. The real exponential function and the exponential map of a matrix are denoted by $\exp(\cdot)$. The Kronecker product of matrices is denoted by $\mathbf{A} \otimes \mathbf{B}$. The 3×3 matrix whose element of row i and column j is equal to one and the remaining elements are zeros is denoted by $\mathbf{E}_{i,j}$. The block diagonal matrix with the elements $\mathbf{A}_1, \dots, \mathbf{A}_n$ in the main block diagonal is expressed as $\text{diag}(\mathbf{A}_1, \dots, \mathbf{A}_n)$. The maximum vector and matrix norms are denoted by $\|\cdot\|_{\max}$ and are defined as the maximum of the absolute value of all vector and matrix elements, respectively, i.e., $\|\mathbf{x}\|_{\max} := \max\{|x_1|, \dots, |x_N|\}$ and $\|\mathbf{A}\|_{\max} := \max\{|\mathbf{A}_{ij}|\}$, where $[\mathbf{A}]_{ij}$

Manuscript received October 11, 2013; revised February 6, 2014, May 29, 2014, September 17, 2014, and October 8, 2014; accepted October 12, 2014. Date of publication October 16, 2014; date of current version June 24, 2015. This work was supported in part by Fundação para a Ciência e a Tecnologia (FCT) [PEst-OE/EEI/LA0009/2013] and by the Fundação para a Ciência e a Tecnologia Ph.D. grant SFRH/BD/47456/2008. Recommended by Associate Editor M. L. Corradini.

S. Brás is with the Laboratory of Robotics and Systems in Engineering and Science (LARSyS), Instituto Superior Técnico, Universidade de Lisboa, Lisbon 1049-001, Portugal (e-mail: sbras@isr.ist.utl.pt).

P. Rosa is with Deimos Engenharia, Lisbon, Portugal (e-mail: paulo.rosa@deimos.com.pt).

C. Silvestre is with the Laboratory of Robotics and Systems in Engineering and Science (LARSyS), Instituto Superior Técnico, Universidade de Lisboa, Lisbon 1049-001, Portugal and also with the Department of Electrical and Computer Engineering, Faculty of Science and Technology of the University of Macau, Taipa, Macau (e-mail: cjs@isr.ist.utl.pt).

P. Oliveira is with the Laboratory of Robotics and Systems in Engineering and Science (LARSyS), and also with the Department of Mechanical Engineering of Instituto Superior Técnico, Universidade de Lisboa, Lisbon 1049-001, Portugal (e-mail: pjcro@isr.ist.utl.pt).

Color versions of one or more of the figures in this paper are available online at <http://ieeexplore.ieee.org>.

Digital Object Identifier 10.1109/TAC.2014.2363300

denotes the element of row i and column j of matrix \mathbf{A} . A polytope is described by a matrix \mathbf{A} and a vector \mathbf{b} such that $\text{Set}(\mathbf{A}, \mathbf{b}) = \{\mathbf{x} \in \mathbb{R}^{n_x} : \mathbf{A}\mathbf{x} \leq \mathbf{b}\}$.

I. INTRODUCTION

The field of Fault Detection and Isolation (FDI) has been studied since the early 70's [1], and several techniques have, since then, been applied to different systems. For a survey of FDI methods in the literature, see, for instance, [2]. An active deterministic model-based Fault Detection (FD) system is usually composed of two parts: a filter that generates residuals that should be *large* under faulty environments; and a decision threshold, which is used to decide whether a fault is present or not—see [1], [3], [4] and references therein. The isolation of the fault can, in some cases, be done using a similar approach, i.e., by designing filters for families of faults, and identifying the most likely fault as the one associated to the filter with the smallest residual. In previous years, new FDI methods have been proposed based on observers—cf. [5]–[8].

The core of a strapdown Inertial Navigation System (INS) is an Inertial Measurement Unit (IMU) comprising rate gyros and accelerometers. When compared with the more traditional gimbaled INS, these systems have the advantage of being mechanically robust, compact, and relatively low-cost. Moreover, adding redundant sensors is more straightforward, which makes the strapdown architecture very attractive for high-reliability navigation systems.

Noise in inertial sensors is typically modeled as a Gaussian and white random variable. As a consequence, many FDI solutions proposed in the literature are based on this stochastic description [9]. In this work, we pursue a distinct approach by considering only upper bounds on the magnitude of the sensor noise. Our approach is deterministic and measurement outliers and sensor readings with very high noise components are directly interpreted as faults.

The FDI schemes for navigation systems available in the literature exploit two types of redundancy, namely, hardware redundancy and analytical or dynamic redundancy. The former takes advantage of the existing redundant measurements to detect incoherences among them—see for instance [10]. The analytical redundancy emerges from the dynamic relationship among the sensor data. The work in [9] proposes two statistical schemes based on nonlinear autoregressive moving average. Several alternative approaches take advantage of the well-known Kalman filtering theory to integrate different sensor measurements and produce the residuals that are used in the FDI decision logic [11], [12].

The main contribution of this work is the development of two FDI schemes for IMUs and vector observations, where the sensor measurements are assumed to be corrupted by bounded noise. We exploit two different types of redundancy: i) hardware redundancy and ii) analytical redundancy. Necessary and sufficient conditions on the magnitude of a fault that ensure detection and isolation of faults using hardware redundancy are established. A preliminary version of

this work appeared in [13]. This work revisits the results of [13] and, in addition, provides: i) necessary conditions for fault isolation with redundant sensors; ii) representative Monte-Carlo simulation results; and iii) a comparison with a standard FDI method based on Kalman filtering.

II. PROBLEM FORMULATION

In this work, we assume that a craft is equipped with a strapdown navigation system comprising an IMU fixed in the body reference frame $\{B\}$. Vector observations, that are fixed in the inertial reference frame $\{I\}$, are also available to mitigate the errors associated with dead reckoning.

A. Measurement Model

We denote the angular velocity of $\{B\}$ with respect to $\{I\}$ and expressed in $\{B\}$ as $\boldsymbol{\omega} \in \mathbb{R}^3$, and the specific force, which is the time-rate-of-change of the velocity of $\{B\}$, with respect to $\{I\}$, relative to a local gravitational space and expressed in $\{B\}$, as $\mathbf{a}_{SF} \in \mathbb{R}^3$ and satisfying $\mathbf{a}_{SF} = {}^B\mathbf{a} - {}^B\mathbf{g}$, where ${}^B\mathbf{a} \in \mathbb{R}^3$ denotes the linear acceleration term and ${}^B\mathbf{g} \in \mathbb{R}^3$ corresponds to the gravity, both expressed in the body-fixed coordinates $\{B\}$.

The IMU is composed of a set of rate gyros and a set of accelerometers. The ideal i -th rate gyro measures the projection of $\boldsymbol{\omega}$ onto its measurement axis, $\mathbf{h}_{\Omega i} \in \mathbb{R}^3$, which is constant in $\{B\}$,

$$\Omega_i = \mathbf{h}_{\Omega i}^T \boldsymbol{\omega} \quad i = 1, \dots, N_{\Omega}. \quad (1)$$

However, the actual rate gyro measurements, Ω_{ri} , are corrupted by bias and noise, which are both assumed to be bounded, i.e.,

$$\Omega_{ri} = \Omega_i + b_i + \delta_{bi} + n_{\Omega i} \quad (2)$$

where $b_i \in \mathbb{R}$ and $n_{\Omega i} \in \mathbb{R}$ denote the measurement bias and noise, respectively, and $|\delta_{bi}| \leq \bar{\delta}_{bi}$. The measurement noise is assumed to be bounded by a positive constant, $|n_{\Omega i}| \leq \bar{n}_{\Omega i}$. The bound $\bar{\delta}_{bi}$ can be seen as a bias tolerance, which reflects the confidence that one has on b_i remaining constant.

Let the measurement axis of the i -th accelerometer be given by $\mathbf{h}_{\alpha i} \in \mathbb{R}^3$, $i = 1, \dots, N_{\alpha}$, which is constant when expressed in $\{B\}$. This sensor ideally measures the projection of the specific force onto its measurement axis $\alpha_i = \mathbf{h}_{\alpha i}^T \mathbf{a}_{SF}$. However, the sensed data are corrupted by bounded sensor noise $\alpha_{ri} = \alpha_i + n_{\alpha i}$, where $n_{\alpha i}$ denotes the measurement noise, which satisfies $|n_{\alpha i}| \leq \bar{n}_{\alpha i}$.

The following assumption guarantees that one can recover $\boldsymbol{\omega}$ and \mathbf{a}_{SF} from $\boldsymbol{\Omega} = [\Omega_1 \dots \Omega_{N_{\Omega}}]^T$ and $\boldsymbol{\alpha} = [\alpha_1 \dots \alpha_{N_{\alpha}}]^T$, respectively.

Assumption 1: The measurement axes of the rate gyros and accelerometers form a basis for \mathbb{R}^3 , i.e., $\text{span}\{\mathbf{h}_{\Omega 1}, \dots, \mathbf{h}_{\Omega N_{\Omega}}\} = \text{span}\{\mathbf{h}_{\alpha 1}, \dots, \mathbf{h}_{\alpha N_{\alpha}}\} = \mathbb{R}^3$.

B. Dynamic Model

To obtain estimates of position and attitude from the inertial data, it is necessary to integrate the measurements. This process introduces cumulative errors in the estimates. To correct them, it is typical to use aiding sensors such as magnetometers, star trackers, and Sun sensors [14]. These sensors measure a vector expressed in $\{B\}$, which, for most practical purposes, can be considered constant in the inertial coordinates $\{I\}$. These vectors satisfy the kinematic equation

$$\dot{\mathbf{v}} = -(\boldsymbol{\omega})_{\times} \mathbf{v} \quad (3)$$

where $\mathbf{v} \in \mathbb{R}^3$ denotes a generic vector observation expressed in $\{B\}$. We assume that the sensors provide measurements of $N_{\mathbf{v}}$ vector observations in the form

$$\mathbf{v}_r^{(i)} = \mathbf{H}_{\mathbf{v}}^{(i)} \mathbf{v}^{(i)} + \mathbf{n}_{\mathbf{v}}^{(i)}, \quad i = 1, \dots, N_{\mathbf{v}} \quad (4)$$

where $\mathbf{H}_{\mathbf{v}}^{(i)}$ is the measurement matrix of vector $\mathbf{v}^{(i)}$, and $\mathbf{n}_{\mathbf{v}}^{(i)}$ is the measurement noise vector. Each component of this vector, denoted by $n_{\mathbf{v}j}^{(i)}$, satisfies

$$\left| n_{\mathbf{v}j}^{(i)} \right| \leq \bar{n}_{\mathbf{v}j}^{(i)} \quad (5)$$

where $n_{\mathbf{v}j}^{(i)}$ denotes the j -th component of the i -th vector observation and $\bar{n}_{\mathbf{v}j}^{(i)} \in \mathbb{R}^+$, $i = 1, \dots, N_{\mathbf{v}}$.

The time derivative of the specific force, $\dot{\mathbf{a}}_{SF}$, is given by

$$\dot{\mathbf{a}}_{SF} = {}^B\dot{\mathbf{a}} - (\boldsymbol{\omega})_{\times} (-{}^B\mathbf{g}) \quad (6)$$

where ${}^B\mathbf{g} \in \mathbb{R}^3$ is the acceleration due to the gravity force expressed in $\{B\}$. However, in many practical applications, the external accelerations can be neglected when compared with gravity. Under this assumption, the norm of the specific force does not change and (6) can be rewritten as

$$\dot{\mathbf{a}}_{SF} \approx -(\boldsymbol{\omega})_{\times} (-{}^B\mathbf{g}) \approx -(\boldsymbol{\omega})_{\times} \mathbf{a}_{SF}.$$

Thus, the specific force has a behavior similar to a vector observation as described in (3), i.e., the measurements of the accelerometers can also be seen as vector observations.

In this work, we follow the characterization of faults described in [15], classifying them into *hard* and *soft* faults. The hard faults include step-type failures, such as zero output and *stuck at* faults. Changes in noise level and bias variation are typical examples of soft faults.

III. FDI USING HARDWARE REDUNDANCY

In this section, a technique to detect faults on sensors by using hardware redundancy is described. The method is detailed for the rate gyros measurements, although it is equally fitted to exploit the redundancy in other sensors, such as accelerometers and magnetometers.

If the sensor redundancy is achieved by using multiple sensors in the same axis, six sensors are required to detect faults and nine are required for the isolation of non-simultaneous faults. Another alternative is to place them in different axis, thereby allowing the detection of faults using only four sensors, while fault isolation is possible using five sensors [16].

From the model of the rate gyros measurements in (2) and the boundedness of the measurement noise, the rate gyro measurements, $\boldsymbol{\Omega}$, satisfy the following (element-wise) inequality

$$\begin{bmatrix} \mathbf{I}_{N_{\Omega}} \\ -\mathbf{I}_{N_{\Omega}} \end{bmatrix} \boldsymbol{\Omega} \leq \begin{bmatrix} \boldsymbol{\Omega}_r - \mathbf{b} + \boldsymbol{\delta}_{\Omega} \\ -\boldsymbol{\Omega}_r + \mathbf{b} + \boldsymbol{\delta}_{\Omega} \end{bmatrix}$$

where $\mathbf{I}_{N_{\Omega}}$ is the $N_{\Omega} \times N_{\Omega}$ identity matrix, $\boldsymbol{\Omega}_r = [\Omega_{r1} \dots \Omega_{rN_{\Omega}}]^T \in \mathbb{R}^{N_{\Omega}}$, $\boldsymbol{\delta}_{\Omega} = [\delta_{\Omega 1} \dots \delta_{\Omega N_{\Omega}}]^T \in \mathbb{R}^{N_{\Omega}}$, $\mathbf{b} = [b_1 \dots b_{N_{\Omega}}]^T \in \mathbb{R}^{N_{\Omega}}$ and

$$\delta_{\Omega i} = \bar{\delta}_{bi} + \bar{n}_{\Omega i}. \quad (7)$$

Therefore,

$$\boldsymbol{\Omega} \in \text{Set}(\mathbf{M}_{\Omega}, \mathbf{m}_{\Omega}) \quad (8)$$

where $\mathbf{M}_{\Omega} = \begin{bmatrix} \mathbf{I}_{N_{\Omega}} \\ -\mathbf{I}_{N_{\Omega}} \end{bmatrix}$, and $\mathbf{m}_{\Omega} = \begin{bmatrix} \boldsymbol{\Omega}_r - \mathbf{b} + \boldsymbol{\delta}_{\Omega} \\ -\boldsymbol{\Omega}_r + \mathbf{b} + \boldsymbol{\delta}_{\Omega} \end{bmatrix}$. Writing (1) in matrix form yields

$$\boldsymbol{\Omega} = \mathbf{H}_{\Omega} \boldsymbol{\omega}. \quad (9)$$

Then, from (8) and (9), it can be concluded that $\boldsymbol{\omega}$ satisfies

$$\boldsymbol{\omega} \in \text{Set}(\mathbf{M}_{\Omega} \mathbf{H}_{\Omega}, \mathbf{m}_{\Omega}). \quad (10)$$

Definition 1: A rate gyro is faulty if its measurements do not satisfy the relations (1) and (2).

Proposition 1: Consider the rate gyros model (2) and the linear transformation between the ideal sensor measurements Ω and the angular velocity ω given in (9). Then, under Assumption 1, if $\text{Set}(\mathbf{M}_\Omega \mathbf{H}_\Omega, \mathbf{m}_\Omega) = \emptyset$, there exists at least one faulty rate gyro.

Proof: Assume that all rate gyros are healthy and that $\text{Set}(\mathbf{M}_\Omega \mathbf{H}_\Omega, \mathbf{m}_\Omega) = \emptyset$. Since all rate gyros are healthy, the rate gyros model (2) holds and $\Omega \in \text{Set}(\mathbf{M}_\Omega, \mathbf{m}_\Omega)$. Then, from the linear transformation (9), we have that $\omega \in \text{Set}(\mathbf{M}_\Omega \mathbf{H}_\Omega, \mathbf{m}_\Omega)$. But this contradicts the initial assumption that $\text{Set}(\mathbf{M}_\Omega \mathbf{H}_\Omega, \mathbf{m}_\Omega) = \emptyset$. Thus, we conclude that there must be at least one faulty sensor. ■

Remark 1: Although the proposed solution requires fixing an upper bound on the sensor noise magnitude and a decision rule based on a limit threshold also depends directly on the sensor noise characteristics [17], the upper bounds to be devised are fixed directly on the sensor space rather than on a more intangible residuals space. Thus, they can be set in a much more straightforward manner, when compared to classical residual-based approaches. Furthermore, the proposed methods are suitable for time-varying bounds, taking into account, for instance, variations in temperature.

The proposed scheme for fault isolation consists in evaluating the emptiness of the polytope $S_i = \text{Set}(\mathbf{M}_{\Omega \setminus \{i\}} \mathbf{H}_{\Omega \setminus \{i\}}, \mathbf{m}_{\Omega \setminus \{i\}})$, where $\mathbf{M}_{\Omega \setminus \{i\}} = [\mathbf{I}_{N_\Omega - 1} \quad -\mathbf{I}_{N_\Omega - 1}]^T$, $\mathbf{H}_{\Omega \setminus \{i\}} = \mathbf{\Gamma}_i \mathbf{H}_\Omega$, $\mathbf{m}_{\Omega \setminus \{i\}} = \text{diag}(\mathbf{\Gamma}_i, \mathbf{\Gamma}_i) \mathbf{m}_\Omega \in \mathbb{R}^{2N_\Omega - 2}$, and $\mathbf{\Gamma}_i = \text{diag}([\mathbf{I}_{i-1} \quad \mathbf{0}_{i-1 \times 1}], \mathbf{I}_{N_\Omega - i})$.

If only for one i , S_i is non-empty, the faulty measurement is Ω_{ri} . If more than one S_i is non-empty, it is not possible to isolate the fault.

Let the model of the faulty rate gyro, $f \in \{1, \dots, N_\Omega\}$, be given by

$$\Omega_{r,f} = \Omega_f + b_f + \delta_{b,f} + n_{\Omega_f} + \varepsilon \quad (11)$$

where $b_f \in \mathbb{R}$, $|\delta_{b,f}| \leq \bar{\delta}_{b,f}$, $|n_{\Omega_f}| \leq \bar{n}_{\Omega_f}$, and $\varepsilon \in \mathbb{R}$ denotes the measurement error resulting from a fault. Moreover, consider all the minimum singular values of the square matrices which columns are three measurement vectors

$$\underline{\sigma}_s = \sigma_{\min}(\mathbf{H}_{ijk}), \quad \mathbf{H}_{ijk} = [\mathbf{h}_i \quad \mathbf{h}_j \quad \mathbf{h}_k]^T$$

where $i \neq j \neq k$, $i \neq k$, $\sigma_{\min}(\cdot)$ denotes the minimum singular value of its argument, and $s = 1, \dots, N_\sigma$, with $N_\sigma = \binom{N_\Omega}{3}$. Additionally, let $\rho \in \mathbb{N}$ be such that $\underline{\sigma}_\rho$ is the minimum non-zero $\underline{\sigma}_s$.

The following proposition provides sufficient conditions on the magnitude of the fault that ensure detection and isolation.

Proposition 2: Assume that there are at least five non-coplanar measurements. Then, if the error associated with a fault satisfies

$$|\varepsilon| > 2\underline{\sigma}_\rho^{-1} \bar{\delta}_\Omega + 2 \max_i \{\delta_{\Omega_i}\} \quad (12)$$

where $\bar{\delta}_\Omega = \max_{\substack{i \neq j, i \neq k \\ k \neq j}} \{\|\delta_{\Omega(ijk)}\|\}$, $\delta_{\Omega(ijk)} = [\delta_{\Omega_i} \quad \delta_{\Omega_j} \quad \delta_{\Omega_k}]^T$, the proposed FDI scheme is guaranteed to detect and isolate non-simultaneous faults.

Proof: The proposed scheme is guaranteed to detect faults if the set compatible with the faulty measurement model does not intersect the set compatible with more than two non-faulty independent measurements. The idea of the proof is to obtain an overbounding ball for the set of points that can be compatible with more than two non-faulty independent measurements, and then provide a condition on the magnitude of the fault that guarantees that the set of points compatible with the faulty measurements does not intersect that ball.

For the sake of comprehension, and without loss of generality, let $\omega = 0$. Then, the measurement model (1), (2) satisfies $\mathbf{h}_i^T \omega \leq \Omega_{ri} - b_i + \delta_{\Omega_i}$ and $-\mathbf{h}_i^T \omega \leq -\Omega_{ri} + b_i + \delta_{\Omega_i}$, where $i = 1, \dots, N_\Omega$. With $\omega = 0$, the following inequality can be derived $|\Omega_{ri} - b_i| \leq \delta_{\Omega_i}$. Thus, all the points compatible with the i -th measurement belong to the set $\Lambda_i = \text{Set}([\mathbf{h}_i \quad -\mathbf{h}_i]^T, 2\delta_{\Omega_i} [1 \quad 1]^T)$.

The points where three hyperplanes limiting the sets Λ_i , Λ_j , and Λ_k intersect satisfy $\mathbf{H}_{ijk} \boldsymbol{\chi} = 2\delta_{\Omega(ijk)}$, and also

$\|\boldsymbol{\chi}\| \leq (2\bar{\delta}_\Omega) / (\sigma_{\min}(\mathbf{H}_{ijk}))$. If one takes the minimum non-zero $\sigma_{\min}(\mathbf{H}_{ijk})$, i.e., σ_ρ , an overbound on the norm of the farthest intersection point, $\boldsymbol{\chi}_\rho$, is obtained, i.e., $\|\boldsymbol{\chi}_\rho\| \leq (2\bar{\delta}_\Omega) / \sigma_\rho$. This overbound is the radius of the ball B_ρ , whose complementary space does not contain any point compatible with more than two non-coplanar measurements.

Now, consider the set compatible with the faulty measurement, which is described by

$$\Lambda_f = \left\{ \boldsymbol{\chi}_f \in \mathbb{R}^3 : \begin{bmatrix} \mathbf{h}_f^T \\ -\mathbf{h}_f^T \end{bmatrix} \boldsymbol{\chi}_f \leq \begin{bmatrix} 2\delta_{\Omega_f} + \varepsilon \\ 2\delta_{\Omega_f} - \varepsilon \end{bmatrix} \right\}. \quad (13)$$

Since there are at least five non-coplanar measurements, if for all $\boldsymbol{\chi}_f \in \Lambda_f$ one has $\|\boldsymbol{\chi}_f\| > \|\boldsymbol{\chi}_\rho\|$, the fault is detected and isolated. From (13) it can be concluded that

$$\begin{cases} \|\boldsymbol{\chi}_f\| \geq -2\delta_{\Omega_f} - \varepsilon \\ \|\boldsymbol{\chi}_f\| \geq -2\delta_{\Omega_f} + \varepsilon \end{cases} \Leftrightarrow \|\boldsymbol{\chi}_f\| \geq -2\delta_{\Omega_f} + |\varepsilon|. \quad (14)$$

Then, by using (12) in (14), it results in $\|\boldsymbol{\chi}_f\| \geq -2\delta_{\Omega_f} + |\varepsilon| > 2\sigma_\rho^{-1} \bar{\delta}_\Omega$, and thus $\|\boldsymbol{\chi}_f\| > \|\boldsymbol{\chi}_\rho\|$. ■

Proposition 2 provides sufficient conditions that ensure detection and isolation. In addition, a necessary condition on the magnitude of the fault for detection and isolation is presented in the following proposition.

Proposition 3: Detection (and isolation) of a fault is only possible if the corresponding fault magnitude satisfies $|\delta_{b,f} + n_{\Omega_f} + \varepsilon| > \delta_{\Omega_f}$.

Proof: To prove this proposition it suffices to show that if

$$|\delta_{b,f} + n_{\Omega_f} + \varepsilon| \leq \delta_{\Omega_f} \quad (15)$$

then, there exists ω such that

$$\begin{bmatrix} \mathbf{I}_{N_\Omega} \\ -\mathbf{I}_{N_\Omega} \end{bmatrix} \mathbf{H}_\Omega \omega \leq \begin{bmatrix} \Omega_r - \mathbf{b} + \delta_\Omega \\ -\Omega_r + \mathbf{b} + \delta_\Omega \end{bmatrix} \quad (16)$$

holds. Without loss of generality, let the faulty sensor be the first and let $\varepsilon = [\varepsilon \ 0 \ \dots \ 0]^T$. Then, from (2) and (11), (16) takes the form

$$\begin{bmatrix} \mathbf{I}_{N_\Omega} \\ -\mathbf{I}_{N_\Omega} \end{bmatrix} \mathbf{H}_\Omega \omega \leq \begin{bmatrix} \Omega + \delta_b + \mathbf{n}_\Omega + \varepsilon + \delta_\Omega \\ -\Omega - \delta_b - \mathbf{n}_\Omega - \varepsilon + \delta_\Omega \end{bmatrix}.$$

From (7) and (15), we have that

$$\begin{bmatrix} \mathbf{I}_{N_\Omega} \\ -\mathbf{I}_{N_\Omega} \end{bmatrix} \mathbf{H}_\Omega \omega \leq \begin{bmatrix} \Omega + \lambda_+ \\ -\Omega + \lambda_- \end{bmatrix} \quad (17)$$

where $\lambda_+ = \delta_b + \mathbf{n}_\Omega + \varepsilon + \delta_\Omega > 0$ and $\lambda_- = -\delta_b - \mathbf{n}_\Omega - \varepsilon + \delta_\Omega > 0$. By taking $\omega = (\mathbf{H}_\Omega^T \mathbf{H}_\Omega)^{-1} \mathbf{H}_\Omega^T \Omega$, it can be concluded that (17) holds, which contradicts the initial assumption, thereby proving the result. ■

Remark 2: The described method is suitable to detect and isolate non-simultaneous faults. To that end, at least five sensors are required. With more sensors and the appropriate modifications, the proposed method may also be suitable to isolate simultaneous faults in two or more sensors.

IV. FDI USING ANALYTICAL REDUNDANCY AND SVOS

In this section, an FDI algorithm based on analytical redundancy is proposed for the case where measurements from rate gyros, and vector observations, are available.

A. Fault Detection

As most physical phenomena, the kinematic model described in (3) is continuous in time and, hence, not in the desired discrete-time framework of the Set-Valued Observers (SVOs). In the following, a

discrete-time approximation of the model based on the knowledge of upper bounds on the magnitude of the angular acceleration is devised.

The exact solution of the differential (3) is given by

$$\mathbf{v}(t) = \exp\left(-\int_{t_0}^t (\boldsymbol{\omega}(\tau))_{\times} d\tau\right) \mathbf{v}(t_0) \quad (18)$$

where $t_0 < t$. Using the Mean Value Theorem twice and (18), we conclude that

$$\mathbf{v}((k+1)T) = \exp\left(-\frac{T^2}{2} (\dot{\boldsymbol{\omega}}(\xi))_{\times} - T (\boldsymbol{\omega}(kT))_{\times}\right) \mathbf{v}(kT) \quad (19)$$

for some $\xi \in [kT, (k+1)T]$, where T denotes the sampling period of the sensor.

In (19), the angular velocity and the angular acceleration are not completely known and hence are not suitable to be used by the SVO. On the other hand, from (10), the angular velocity satisfies

$$\boldsymbol{\omega}(kT) \in \text{Set}(\mathbf{M}_{\boldsymbol{\omega}}(kT), \mathbf{m}_{\boldsymbol{\omega}}(kT)) \quad (20)$$

where $\mathbf{M}_{\boldsymbol{\omega}}(kT) = \mathbf{M}_{\Omega}(kT)\mathbf{H}_{\Omega}$ and $\mathbf{m}_{\boldsymbol{\omega}}(kT) = \mathbf{m}_{\Omega}(kT)$. Since (20) defines a convex polytope, the center of the polytope, denoted by $\boldsymbol{\omega}_r(kT)$, can be computed by resorting to a linear optimization problem. Define $\bar{\omega}_r = \|\boldsymbol{\omega}_r(kT)\|_{\max}$, and let us denote the uncertainty in the angular velocity as $\boldsymbol{\delta}_{\boldsymbol{\omega}}(kT)$, such that

$$\boldsymbol{\delta}_{\boldsymbol{\omega}}(kT) = \boldsymbol{\omega}(kT) - \boldsymbol{\omega}_r(kT). \quad (21)$$

Note that the uncertainty $\boldsymbol{\delta}_{\boldsymbol{\omega}}(kT)$ satisfies $\boldsymbol{\delta}_{\boldsymbol{\omega}}(kT) \in \text{Set}(\mathbf{M}_{\boldsymbol{\omega}}(kT), \mathbf{m}_{\boldsymbol{\omega}}(kT) - \mathbf{M}_{\boldsymbol{\omega}}(kT)\boldsymbol{\omega}_r(kT))$, which denotes a polytope centered at the origin and let the maximum distance along any major axis to the boundary of this polytope be given by

$$\bar{\delta}_{\boldsymbol{\omega}} = \|\boldsymbol{\delta}_{\boldsymbol{\omega}}(kT)\|_{\max}. \quad (22)$$

The angular acceleration is inherently bounded due to the limitations in terms of the energy that characterize any physical system. Moreover, in many applications, either due to constraints on the thrusters, or due to the action of friction, it is in fact possible to derive an upper bound on the magnitude of the angular acceleration. Hence, we pose the following assumption.

Assumption 2: Assume that the magnitude of the angular acceleration is bounded by a known (but possibly conservative) positive scalar $\bar{\phi}_{\boldsymbol{\omega}}$, i.e.,

$$\|\dot{\boldsymbol{\omega}}\|_{\max} \leq \bar{\phi}_{\boldsymbol{\omega}}, \quad \bar{\phi}_{\boldsymbol{\omega}} \in \mathbb{R}^+. \quad (23)$$

For simplicity of notation, in the remainder of this work the time dependence of the variables will be simply denoted by k , $k \in \mathbb{N}$.

Using the result in [18, Appendix A] and the magnitude bounds on the uncertainty of the angular velocity measurements (23) and on the angular acceleration (21), we derive the following relation for each element of the dynamic matrix:

$$\begin{aligned} & \left[\exp\left(-T\left(\boldsymbol{\omega}_r(k) + \frac{T}{2}\dot{\boldsymbol{\omega}}(\xi) + \boldsymbol{\delta}_{\boldsymbol{\omega}}(k)\right)_{\times}\right) \right]_{ij} \\ & = \left[\exp\left(-T\left(\boldsymbol{\omega}_r(k)\right)_{\times}\right) \right]_{ij} + \epsilon \Delta_{(i,j)}(k) \end{aligned}$$

for some $|\Delta_{(i,j)}(k)| \leq 1$, where

$$\epsilon = \frac{1}{2} \left(\exp\left(2T\left(\bar{\omega}_r + \bar{\delta}_{\boldsymbol{\omega}} + \frac{T}{2}\bar{\phi}_{\boldsymbol{\omega}}\right)\right) - \exp(2T\bar{\omega}_r) \right). \quad (24)$$

With this construction, we have obtained a discrete-time approximate system that depends solely on sensor data and is in the framework of the SVOs [19], [20]. The upper bound on the approximation error,

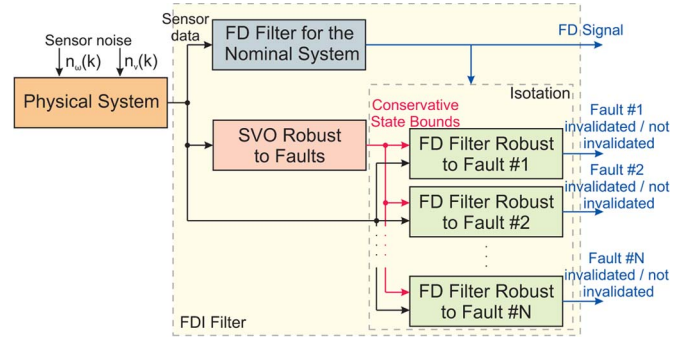


Fig. 1. Proposed fault detection and isolation (FDI) filter for navigation systems.

ϵ , can be handled by the same framework. Hence, an SVO can be designed to the system

$$\begin{cases} \mathbf{x}(k+1) = \mathbf{A}_0(k)\mathbf{x}(k) + \mathbf{A}_{\Delta}(k)\mathbf{x}(k) \\ \mathbf{y}(k) = \mathbf{C}(k)\mathbf{x}(k) + \mathbf{n}(k) \end{cases} \quad (25)$$

where $\mathbf{x}(k+1) = [\mathbf{v}^{(1)T} \dots \mathbf{v}^{(Nv)T}]^T$, $\mathbf{A}_0(k) = \mathbf{I}_{Nv} \otimes \exp(-T(\boldsymbol{\omega}_r(k))_{\times})$, $\mathbf{C}(k) = \text{diag}(\mathbf{H}_v^{(1)}, \dots, \mathbf{H}_v^{(Nv)})$, $\mathbf{n} = [\mathbf{n}_v^{(1)T} \dots \mathbf{n}_v^{(Nv)T}]^T$, $\mathbf{A}_{\Delta}(k) = \sum_{i=1}^N \mathbf{A}_i(k)\Delta_{(m,n)}(k)$, $i = 1, \dots, N$, where $|\Delta_{(m,n)}(k)| \leq 1$ are unknown variables and $\mathbf{A}_i(k) = \mathbf{I}_{Nv} \otimes \epsilon \mathbf{E}_{m,n}$, $m = 1, \dots, 3$, $n = 1, \dots, 3$, $i = m + 3(n-1)$.

If, at some point, the set containing the state, $\text{Set}(\mathbf{M}(k), \mathbf{m}(k))$, degenerates into the empty set, we conclude that the model no longer describes the system and sensor data, and hence a fault has occurred. The main property of the proposed FD architecture is formally stated in the following proposition.

Proposition 4: Consider the model of the rate gyros (2) and the model of the vector observations (4), which are dynamically related by the model (3), and the corresponding SVO described in (25). Then, if $\text{Set}(\mathbf{M}(k), \mathbf{m}(k)) = \emptyset$, for some $k \geq 0$, a fault has occurred at some time instant $k_f \leq k$. The proof of this proposition is omitted as it follows directly from the construction in this section.

Remark 3: The proposed FD filter guarantees that there will be no false alarms. However, it may not be able to detect some sensor faults. This may be due to severe sensor noise or to the conservatism added to the model in (25). This problem is related with the concept of indistinguishability. The interested reader is referred to [21].

Remark 4: This method might not be suitable for systems with very low computational power. However, nowadays, many aircrafts and other vehicles equipped with IMUs have available onboard powerful state-of-the-art computers. In addition, the proposed solution is highly parallelizable.

B. Fault Isolation

In this work, we adopt the strategy proposed in [22] and illustrated in Fig. 1, which relies on the concept of model invalidation. A bank of SVOs is designed modeling each different fault, and another SVO is synthesized modeling the nominal (non-faulty) system. Under certain distinguishability conditions, only one model is consistent with the sensor data, and thus all the others SVOs will be invalidated, i.e., their set-valued state estimates will degenerate into the empty set. The remaining SVO, if any, isolates the fault.

To spare unnecessary computational burden, and since faults can occur at any time, we use the following scheme. Firstly, only the nominal FD filter and one SVO robust to all faults are active. The set estimated by the robust SVO is designed to always include the true state of the system, even if a fault in the sensors has occurred. If, at some point, the FD filter for the nominal system is invalidated,

it indicates that a fault has occurred. Hence, the bank of FD filters modeling the faults is initialized with the set estimated by the robust SVO. Once all the filters describing faults that did not occur have been invalidated, we have isolated the fault.

1) *Faults in the Vector Observations:* The faults in the vector observations can be modeled directly in an SVO. The hard faults considered are the zero output and the *stuck at* types of faults. The zero output fault is modeled by zeroing the row in the measurement matrix corresponding to the faulty sensor, whereas a *stuck at* type of fault is modeled by considering that the sensor model is given by $v_{rj}^{(i)}(k+1) = v_{rj}^{(i)}(k)$, for some $i = 1, \dots, N_v$. Thus, the SVO for this fault performs the intersection of the set obtained from the measurements that contains $v_{rj}^{(i)}$ at successive time instants, neglecting the dynamics of the system (for this sensor). The soft faults are modeled by an unexpected increase in the magnitude of the sensor noise, i.e., a larger value $\bar{n}_{v_i}^{(j)}$ in (5).

2) *Faults in the Rate Gyros:* The kinematics of the rigid body attitude depends nonlinearly on the angular velocity. For that reason, this method can accurately determine that a fault has occurred in one of the rate gyros. However, it may not be able to isolate the faulty rate gyro. A higher noise magnitude in the rate gyros bias is modeled by using an SVO with larger value of $\bar{\delta}_\omega$ in (22). A bias variation greater than what was anticipated can be modeled by a larger value of δ_{b_i} in (7) and, consequently, a larger value of $\bar{\delta}_\omega$ in (24). Since these two sources of uncertainty influence the dynamics in a similar way, they are indistinguishable in the sense of [21]. As a consequence, we can only design an SVO that is tolerant to both faults. To model a hard fault in the rate gyros, it is necessary to design a particular SVO for the faulty rate gyro measurement assuming the model $\Omega_i(k+1) = \Omega_i(k)$.

Remark 5: The proposed method for fault isolation using analytical redundancy is based on model invalidation of each of the faults. Thus, like in other methods based on the same approach, the number of models required to consider combinations of faults may render the necessary computational resources impractical.

V. SIMULATIONS RESULTS

In this section, Monte-Carlo simulations have been carried out to assess the performance of the two proposed FDI schemes. The number of iterations necessary for detection and isolation of faults are evaluated for 100 runs. We consider a scenario with five rate gyros, and two vector observations, each of which with five sensors, with installation matrices described by

$$\mathbf{H}_\Omega = \mathbf{H}_v^{(1)} = \mathbf{H}_v^{(2)} = \begin{bmatrix} 1 & 0 & 0 \\ 0 & 1 & 0 \\ 0.47 & 0.47 & 0.75 \\ -0.64 & 0.17 & 0.75 \\ 0.17 & -0.64 & 0.75 \end{bmatrix}.$$

We assume that the sensors are installed onboard a vehicle describing oscillatory angular movements. Under normal operation, the rate gyros measurements are corrupted by noise with uniform distribution over the interval $[-0.573 \ 0.573]$ deg s⁻¹ and for the bias calibrated at the beginning of the mission, we assume a tolerance of $|\bar{\delta}_b^{(i)}| = 0.0115$ deg s⁻¹, $i = 1, \dots, 5$. Each vector observation is normalized, and each sensor measurement is corrupted by (normalized) noise with uniform distribution over the interval $[-0.05 \ 0.05]$. The sampling period of all sensors is $T = 0.1$ s. We assume that one of the following six faults can occur: 1) a *stuck at* type of fault in rate gyro #1; 2) rate gyro #3 badly damaged generating a null measurement; 3) the maximum amplitude of the noise in the rate gyro #3 increases fifteen times; 4) a *stuck at* type of fault in first sensor of vector #1; 5) the second component of vector #2 is null; 6) the maximum amplitude of the noise in the third sensor of vector #3 increases five times.

TABLE I
MEAN (μ) AND STANDARD DEVIATION (σ) OF THE NUMBER OF ITERATIONS NECESSARY TO DETECT AND ISOLATE THE FAULTS AND PERCENTAGE OF CORRECT ISOLATIONS (% C. I.)

#	k_d HW	k_i HW	%	k_d An.	k_i An.	%
	μ (σ)	μ (σ)	C. I.	μ (σ)	μ (σ)	C. I.
1	0.9 (0.5)	4.2 (1.2)	100	1.9 (0.5)	2.9 (0.8)	100
2	0.0 (0.0)	0.0 (0.0)	100	1.0 (0.0)	1.5 (0.8)	100
3	0.3 (0.6)	0.5 (0.7)	100	1.3 (0.6)	1.9 (1.1)	100
4	16.3 (2.6)	23.7 (2.2)	100	13.1 (4.1)	15.1 (3.3)	100
5	1.7 (1.1)	10.0 (2.8)	100	0.0 (0.0)	1.3 (0.7)	100
6	1.6 (2.0)	6.2 (5.5)	100	0.5 (0.7)	1.3 (1.2)	100
#	k_d Proj.	k_i Proj.	%	k_d KF.	k_i KF.	%
	μ (σ)	μ (σ)	C. I.	μ (σ)	μ (σ)	C. I.
1	13.1 (1.0)	14.3 (1.17)	100	0.5 (2.0)	0.5 (2.0)	95
2	0.0 (0.0)	0.1 (0.34)	100	0.6 (2.0)	0.6 (2.0)	95
3	-	-	0	26.3 (8.6)	26.3 (8.6)	0
4	20.4 (1.1)	20.8 (1.2)	100	3.2 (2.9)	3.2 (2.9)	95
5	5.3 (0.9)	6.1 (1.3)	100	0.0 (1.9)	0.0 (1.9)	95
6	19.1 (30.1)	52.0 (51.1)	100	3.5 (4.3)	3.5 (4.3)	77

Table I provides the mean and the standard deviation of number of iterations, i.e., the number of sampling periods, required to detect and isolate each fault and in terms of the ratio of correct isolations using the proposed methods exploiting hardware redundancy (HW) and analytical redundancy (An.). The results obtained with two alternative FDI methods are included. One exploits the hardware redundancy and is based on the projection of the measurement vector onto the orthogonal complement of the range space of the system matrix (Proj.) [10], whereas the second one exploits the analytical redundancy using a bank of Kalman filters (KF), as described in [12]. In this table, k_d and k_i stand for the number of iterations required for detection and isolation, respectively.

The results presented in Table I show that the proposed methods are able to detect and isolate the considered faults. It should be noted that, even with a sampling time of $T = 0.1$ s, the two proposed methods are, on average, able to detect and isolate all the tested faults in less than 2.5 s (25 iterations). For this scenario, in most cases, the proposed methods (HW and An.) detect and isolate faults in less iterations than the Proj. and KF-based methods, even after considerable tuning effort. In the KF-based method (proposed in [12]), a fault is simultaneously detected and isolated. Thus, the values k_d and k_i obtained with this method are similar. Fault #4 takes more time to be detected and isolated by the proposed methods than the remaining faults and also takes some time to be detected and isolated by the Proj. and KF-based methods. When this fault occurs, the time derivative of the sensor measurement is almost zero. Since the fault is characterized by the sensor measurement being *stuck at* a constant value, the faulty measurements and its nominal value are initially very similar to one another, which hinders its detection. It is also remarked that the KF-based method is not able to correctly isolate fault #3, while the Proj. method cannot detect it. Moreover, the KF-based method sometimes isolated the remaining faults incorrectly.

VI. CONCLUSION

In this work, we proposed two novel FDI methodologies for IMUs and vector observations. The first scheme takes advantage of hardware redundancy in the sensor measurements to detect incoherences between them. Necessary and sufficient conditions have been provided that guarantee detection and isolation of non-simultaneous faults. To exploit the dynamic relation between the angular velocity and the vector measurements, a second methodology was proposed based on set-valued state estimates provided by SVOs, which can be used to validate or falsify different models of faults. This method has, however, the disadvantage of requiring more computational power. Neither

solution generates false detections, as long as the non-faulty model of the system remains valid. In addition, due to the set-based construction of the methods, the tuning of a decision threshold is not necessary.

REFERENCES

- [1] A. Willsky, "A survey of design methods for failure detection in dynamic systems," *Automatica*, vol. 12, pp. 601–611, 1976.
- [2] I. Hwang, S. Kim, Y. Kim, and C. Eng Seah, "A survey of fault detection, isolation and reconfiguration methods," *IEEE Trans. Control Syst. Technol.*, vol. 18, no. 3, pp. 636–653, 2010.
- [3] J. Bokor and G. Balas, "Detection filter design for LPV systems—A geometric approach," *Automatica*, vol. 40, pp. 511–518, 2004.
- [4] S. Narasimhan, P. Vachhani, and R. Rengaswamy, "New nonlinear residual feedback observer for fault diagnosis in nonlinear systems," *Automatica*, vol. 44, pp. 2222–2229, 2008.
- [5] H. Hammouri, M. Kinnaert, and E.-H. El Yaagoubi, "Observer-based approach to fault detection and isolation for nonlinear systems," *IEEE Trans. Autom. Control*, vol. 44, no. 10, pp. 1879–1884, Oct. 1999.
- [6] C. De Persis and A. Isidori, "A geometric approach to nonlinear fault detection and isolation," *IEEE Trans. Autom. Control*, vol. 46, no. 6, pp. 853–865, Jun. 2001.
- [7] S. Longhi and A. Monteriu, "Fault detection for linear periodic systems using a geometric approach," *IEEE Trans. Autom. Control*, vol. 54, no. 7, pp. 1637–1643, Jul. 2009.
- [8] P. Zhang, S. Ding, and P. Liu, "A lifting based approach to observer based fault detection of linear periodic systems," *IEEE Trans. Autom. Control*, vol. 57, no. 2, pp. 457–462, Feb. 2012.
- [9] D. Dimogianopoulos, J. Hios, and S. Fassois, "FDI for aircraft systems using stochastic pooled-NARMAX representations: Design and assessment," *IEEE Trans. Control Syst. Technol.*, vol. 17, no. 6, pp. 1385–1397, Nov. 2009.
- [10] D. Skoogh and A. Lennartsson, "A method for multiple fault detection and isolation of redundant inertial navigation sensor configurations," in *Proc. IEEE/ION 2006 Position, Location, And Navigation Symp.*, 2006, pp. 415–425.
- [11] M. Carminati, G. Ferrari, R. Grassetti, and M. Sampietro, "Real-time data fusion and MEMS sensors fault detection in an aircraft emergency attitude unit based on Kalman filtering," *IEEE Sensors J.*, vol. 12, no. 10, pp. 2984–2992, 2012.
- [12] P. Maybeck, "Multiple model adaptive algorithms for detecting and compensating sensor and actuator/surface failures in aircraft flight control systems," *Int. J. Robust and Nonlin. Control*, vol. 9, no. 14, pp. 1051–1070, 1999.
- [13] S. Brás, P. Rosa, C. Silvestre, and P. Oliveira, "Fault detection and isolation for inertial measurement units," in *Proc. 51st IEEE Conf. Decision and Control and European Control Conf.*, Maui, HI, USA, Dec. 2012.
- [14] J. Farrell, *Aided Navigation: GPS With High Rate Sensors*, 1st ed. New York: McGraw-Hill, 2008.
- [15] P. Maybeck and R. Stevens, "Reconfigurable flight control via multiple model adaptive control methods," *IEEE Trans. Aerosp. Electron. Syst.*, vol. 27, no. 3, pp. 470–480, May 1991.
- [16] M. Sturza, "Navigation system integrity monitoring using redundant measurements," *J. Inst. Navigation*, vol. 35, no. 4, pp. 69–87, 1988.
- [17] M. Blanke, J. Schröder, M. Kinnaert, J. Lunze, and M. Staroswiecki, *Diagnosis and Fault-Tolerant Control*. New York, NY, USA: Springer, 2006.
- [18] S. Brás, P. Rosa, C. Silvestre, and P. Oliveira, "Set-valued observers for attitude and rate gyro bias estimation," in *Proc. 2012 American Control Conf.*, Montreal, Canada, Jun. 2012, pp. 1098–1103.
- [19] M. Milanese and A. Vicino, "Optimal estimation theory for dynamic systems with set membership uncertainty: An overview," *Automatica*, vol. 27, no. 6, pp. 997–1009, 1991.
- [20] J. Shamma and K.-Y. Tu, "Set-valued observers and optimal disturbance rejection," *IEEE Trans. Autom. Control*, vol. 44, no. 2, pp. 253–264, 1999.
- [21] P. Rosa and C. Silvestre, "On the distinguishability of discrete linear time-invariant dynamic systems," in *Proc. 50th IEEE Conf. Decision and Control and European Control Conf.*, Orlando, FL, USA, Dec. 2011.
- [22] P. Rosa, C. Silvestre, J. Shamma, and M. Athans, "Fault detection and isolation of LTV systems using set-valued observers," in *Proc. 49th IEEE Conf. Decision and Control*, Dec. 2010.